

GaSb based light emitting diodes with strained InGaAsSb type I quantum well active regions

Sergey Suchalkin,^{1,a)} Seungyong Jung,² Gela Kipshidze,² Leon Shterengas,² Takashi Hosoda,² David Westerfeld,¹ Donald Snyder,³ and Gregory Belenky²

¹Power Photonic Corporation, Stony Brook, New York 11790, USA

²State University of New York at Stony Brook, Stony Brook, New York 11794, USA

³Air Force Research Laboratory, Eglin Air Force Base, Florida 32542, USA

(Received 2 July 2008; accepted 29 July 2008; published online 26 August 2008)

Mid-IR ($\lambda \approx 3\text{--}3.5 \mu\text{m}$) light emitting diodes with quinary AlInGaAsSb barriers and InGaAsSb strained quantum wells grown on GaSb substrates have been demonstrated. The devices produced a quasi-cw emission power of 0.7 mW at room temperature and 2.5 mW at $T=80 \text{ K}$. © 2008 American Institute of Physics. [DOI: 10.1063/1.2974795]

Light emitting diodes (LEDs) operated at room temperature in the $3\text{--}3.5 \mu\text{m}$ spectral range are important for a variety of military and civilian applications (e.g., gas sensing, molecular spectroscopy, chemical process monitoring, and mid-IR imaging). Type I LEDs with bulk active regions grown by liquid phase epitaxy (LPE) on InAs or GaSb cover the spectral range from 1.6 to $4.6 \mu\text{m}$.^{1,2} A continuous wave (cw) output power of $\sim 100 \mu\text{W}$ at $\lambda=3.4 \mu\text{m}$ was demonstrated.³ InAs based type I emitters with single InAsSb quantum wells (QWs) operated at 5 and $8 \mu\text{m}$ and produced 50 and $24 \mu\text{W}$ of cw power at $T=300 \text{ K}$.⁴ Type II cascaded interband heterostructures grown by molecular beam epitaxy (MBE) have also been used to develop mid-IR emitters in the $3\text{--}8 \mu\text{m}$ spectral range.^{5,6}

Good hole localization can be problematic for AlGaAsSb/InGaAsSb LEDs operating at wavelengths above $2.3 \mu\text{m}$. Devices operating above $3 \mu\text{m}$ with an In concentration in the QW above 50% require a QW As concentration over 20% to keep the QW strain below 1.6%–1.9%. The increased As concentration leads to a strong reduction of hole confinement resulting in degraded performance at higher temperatures. To compensate for this we evaluated two different approaches for improved hole confinement. In the first approach, we reduced the Al content in the AlGaAsSb barrier to 35% and in the second approach we employed a quinary AlInGaAsSb barrier in the LED design. The quinary alloy provides an additional degree of freedom allowing for independent control of strain and valence band offset. In both cases⁷ hole confinement was restored due to an increase in the valence band offset between the barrier and the QW.

The LED structures were grown at Stony Brook on GaSb substrates using a Veeco GEN930 MBE system. Four compressively (1.7%–1.9%) strained InGaAsSb QWs separated by 40 nm were incorporated into the AlGaAsSb or AlInGaAsSb barriers (Table I). The emission wavelength was controlled by adjusting the In content in the QW material and the QW width. The active region was sandwiched between doped layers of either $\text{Al}_{0.9}\text{GaAs}_{0.07}\text{Sb}$ or $\text{Al}_{0.6}\text{GaAs}_{0.05}\text{Sb}$ to form the diode structure (Fig. 1). The substrate was *n*-doped with Te to $(2\text{--}3) \times 10^{17} \text{ cm}^{-3}$, and the epitaxial side was *p*-doped with Be to $2 \times 10^{18} \text{ cm}^{-3}$. A 50 nm thick Be doped *p*+GaSb cap was grown on top of the structure.

The LEDs were fabricated as described below into either 3×3 or 4×5 arrays of $100 \times 100 \mu\text{m}^2$ LEDs (Fig. 1). The epilayer side of the wafer was first covered with a $0.3 \mu\text{m}$ thick silicon nitride dielectric layer. Square windows of $100 \times 100 \mu\text{m}^2$ were then opened in the dielectric. A Ti:Au *p*-contact metallization was then deposited onto the entire epilayer side. All of the individual LEDs shared the same metallization, and the devices could not be independently operated. The substrate was lapped and polished to a final thickness of $100 \mu\text{m}$. Stripes of *n*-contacts were deposited onto the substrate side. The stripe contact configuration does not obscure the LEDs when the devices are mounted epi side down so that the light can be extracted through the substrate. No special arrangements such as surface texturing were made to increase the outcoupling efficiency of the devices.

Room temperature electroluminescence spectra for the different devices were measured under 50% duty cycle operation using a Fourier transform infrared spectrometer

TABLE I. The parameters of the device structures.

Device	Cladding	Barrier	QW	No. of QWs (nm)	QW width (nm)
1	$\text{Al}_{0.9}\text{GaAs}_{0.07}\text{Sb}$	$\text{Al}_{0.35}\text{GaAs}_{0.03}\text{Sb}$	$\text{In}_{0.55}\text{GaAs}_{0.22}\text{Sb}$	10	12
2	$\text{Al}_{0.6}\text{GaAs}_{0.05}\text{Sb}$	$\text{Al}_{0.2}\text{In}_{0.25}\text{GaAs}_{0.24}\text{Sb}$	$\text{In}_{0.54}\text{GaAs}_{0.24}\text{Sb}$	4	17
3	$\text{Al}_{0.6}\text{GaAs}_{0.05}\text{Sb}$	$\text{Al}_{0.2}\text{In}_{0.2}\text{GaAs}_{0.2}\text{Sb}$	$\text{In}_{0.54}\text{GaAs}_{0.24}\text{Sb}$	4	17
4	$\text{Al}_{0.9}\text{GaAs}_{0.07}\text{Sb}$	$\text{Al}_{0.35}\text{GaAs}_{0.03}\text{Sb}$	$\text{In}_{0.55}\text{GaAs}_{0.22}\text{Sb}$	5	12

^{a)}Electronic mail: suchal@ece.sunysb.edu.

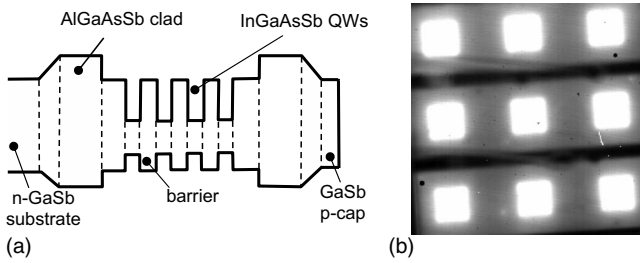


FIG. 1. Schematic band of the LED (a) and a mid-IR image of a LED array at room temperature ($I=100$ mA, b).

(Fig. 2). As the temperature decreases from 300 to 80 K, the maximum of each spectrum shifts toward shorter wavelengths at a rate of ~ 2.3 nm/K. The shorter wavelength of device 1 is possibly due to blueshift caused by increased exposure to high temperature during the structure growth. The device voltage and series resistance increase as the temperature decreases from 200 to 80 K (Fig. 2). This may be due to a reduced carrier concentration in the claddings or barriers at lower temperatures.

The output power of the LED arrays was measured using an InSb photovoltaic detector, a preamplifier, and a lock-in amplifier. An integrating sphere with a 1 in. input aperture in close proximity to the device was used to increase the collection angle to include almost the entire hemisphere. The integrating sphere also acts to homogenize the output emission for reduced sensitivity to optical alignment and improved optical power measurement accuracy. The system was calibrated using a Molectron power meter and a mid-IR interband cascade laser operating at $3.4 \mu\text{m}$. The dependence of output power on bias current for device 2 at several dif-

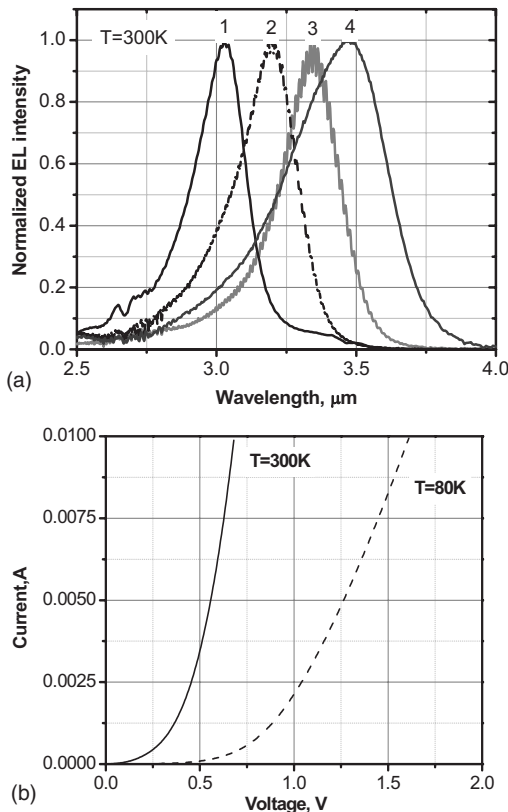


FIG. 2. Electroluminescence spectra, 50% duty cycle, 3 kHz frequency, $T=300$ K (a), and voltage-current dependencies (b).

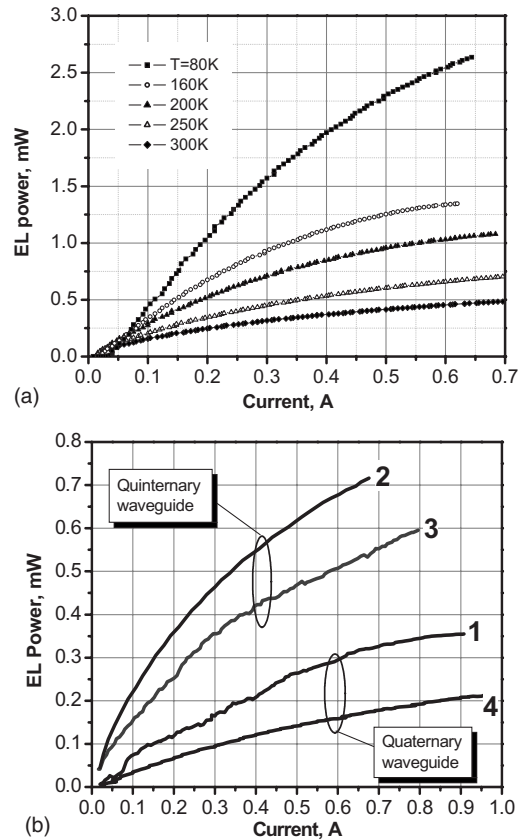


FIG. 3. The dependence of light power on injected current of device 2 (a) and output power vs injected current for devices with quaternary and quinternary barriers (b).

ferent temperatures and the dependence of output power on bias current for each of the four devices at one fixed temperature are both presented in Fig. 3. Measurements were made at a 50% duty cycle and a 3 kHz pulse repetition rate. The sublinear character of the curves in Fig. 3 is caused by a combination of device heating, increased Auger recombination, and overflowing of the QWs accompanied by enhanced leakage. We can estimate the internal quantum efficiency of the devices using the following expression:

$$\eta_{\text{internal}} = 100\% \times \frac{Pe}{IE_{\text{photon}}} \left(\frac{100\%}{\eta_{\text{injection}}} \right) \left(\frac{100\%}{\eta_{\text{extraction}}} \right), \quad (1)$$

where P is the measured power, e is the electron charge, I is the bias current, E_{photon} is the photon energy, $\eta_{\text{injection}}$ is the injection efficiency, and $\eta_{\text{extraction}}$ is the light extraction efficiency (limited by the escape cone). For a rough estimation we can take $\eta_{\text{injection}}$ as 40%—this number was obtained for lasers of similar design.⁷ Since no special measures were taken to increase light outcoupling efficiency, $\eta_{\text{extraction}}$ can be estimated using the following expression:⁸

$$\eta_{\text{extraction}} \approx \frac{n_{\text{air}}^2}{4n_s^2} T, \quad (2)$$

where n_{air} and n_s are the effective refraction indices of air and the LED material, and $T \sim 0.7$ is the Fresnel transmission coefficient. Taking into account the light reflection from the bottom contact we can estimate $\eta_{\text{extraction}}$ as $\sim 3\%$. Solving for the internal quantum efficiency gives $\eta_{\text{internal}} \approx 17\%$ at $I=0.7$ A and 300 K for device 2. The difference in output power between LEDs with quaternary and quinternary

barriers most probably originates from the improved injection efficiency in the quaternary LEDs. A more detailed study of the effect of barrier material on LED performance will be published in another work. The maximum registered output powers were ~ 2.5 mW (0.6 A) at 80 K and 0.7 mW (0.7 A) at 300 K at a duty cycle of 50%. The highest optical power was obtained from device 2, a quaternary $3.13 \mu\text{m}$ LED (Fig. 3).

In conclusion, we presented the electroluminescent properties of GaSb based MBE grown LEDs with quaternary AlGaAsSb and quaternary AlInGaAsSb barriers and strained InGaAsSb QWS. An optical power of 2.5 mW was obtained at 80 K and 0.6 A. At room temperature the output power was 0.7 mW at 0.7 A at a wavelength of $3.13 \mu\text{m}$. The estimated internal quantum efficiency of this device was $\sim 17\%$ ($I=0.7$ A, $T=300$ K). The outcoupling efficiency and output power of the LEDs can be further increased by thinning and patterning the substrate surface or by the application of immersion lenses.

The authors wish to acknowledge the support of the United States Air Force under Contract No. FA8651-07-C-0152, and of the National Science Foundation under Grant No. DMR0710154.

- ¹A. Krier, *Philos. Trans. R. Soc. London, Ser. A* **359**, 599 (2001).
- ²B. A. Matveev, M. Aydaraliev, N. V. Zotova, S. A. Karandashov, N. D. Il'inskaya, M. A. Remennyi, N. M. Stus, and G. N. Talalakin, *IEE Proc.: Optoelectron.* **150**, 356 (2003).
- ³N. V. Zotova, N. D. Il'inskaya, S. A. Karandashev, B. A. Matveev, M. A. Remennyi, and N. M. Stus, *Semiconductors* **40**, 697 (2006).
- ⁴P. J. P. Tang, H. Hardaway, J. Heber, C. C. Phillips, M. J. Pullin, R. A. Stradling, W. T. Yuen, and L. Hart, *Appl. Phys. Lett.* **72**, 3473 (1998).
- ⁵N. C. Das, *Appl. Phys. Lett.* **90**, 011111 (2007).
- ⁶R. Q. Yang, C. H. Lin, S. J. Murry, S. S. Pei, H. C. Liu, M. Buchanan, and E. Dupont, *Appl. Phys. Lett.* **70**, 2013 (1997).
- ⁷T. Hosoda, G. Belenky, L. Shterengas, G. Kipshidze, and M. V. Kisin, *Appl. Phys. Lett.* **92**, 091106 (2008).
- ⁸E. F. Schubert, *Light-Emitting Diodes* (Cambridge University Press, Cambridge, 2003).